Structural Determination of Thermally and Hydrazine Treated Graphene Oxide Using Electron Spectroscopic Analysis

ARTICLE *in* THE JOURNAL OF PHYSICAL CHEMISTRY C · SEPTEMBER 2013

Impact Factor: 4.77 · DOI: 10.1021/jp405682u

4 AUTHORS, INCLUDING:

Amanda V Ellis
Flinders University
147 PUBLICATIONS **1,927** CITATIONS
SEE PROFILE

Habib Dalal
University of Adelaide
8 PUBLICATIONS **25** CITATIONS
SEE PROFILE

THE JOURNAL OF PHYSICAL CHEMISTRY C

Article

pubs.acs.org/JPCC

Structural Determination of Thermally and Hydrazine Treated Graphene Oxide Using Electron Spectroscopic Analysis

Amanda V. Ellis, Altaf Al-deen, Habibullah Dalal, and Gunther G. Andersson*

Flinders Centre for NanoScale Science and Technology, Flinders University, Sturt Road, Bedford Park, Adelaide SA 5042, Australia

ABSTRACT: Here we use UV photoelectron spectroscopy (UPS) and metastable induced electron spectroscopy (MIES) to determine the valence electron structure of graphene oxide (GO) and hydrazine modified graphene oxide, or so-called reduced GO (rGO). We show that pristine GO has a low density of states (DOS) in the $2p\pi$ region. Upon thermal treatment, under vacuum, to 200 °C, the DOS in the $2p\pi$ region increase. The change in the DOS is also reflected in a change in the functional groups attached to the GO. These changes are followed by X-ray photoelectron spectroscopy (XPS). Based on the XPS measurements, the GO is described as highly carboxylated, much akin to pyromellite, with incorporated benzoquinone moieties. After heat treatment to 100 °C, we propose the close proximity of the pendant carboxyls undergoes a condensation reaction to form dianhydrides such that the graphene sheet now consists of a mixture of dianhydride, phthalate-type carboxyl, and benzoquinone moieties with the work function increasing to 4.8 ± 0.1 eV. With further heating to 200−300 °C, these groups are cleaved and the work function decreases back to 4.2 ± 0.1 eV. Lastly, the rGO is shown to form pyrazoline-type bonds with an interrupted 2pπ graphene network which results in a decreased work function to 3.4 eV.

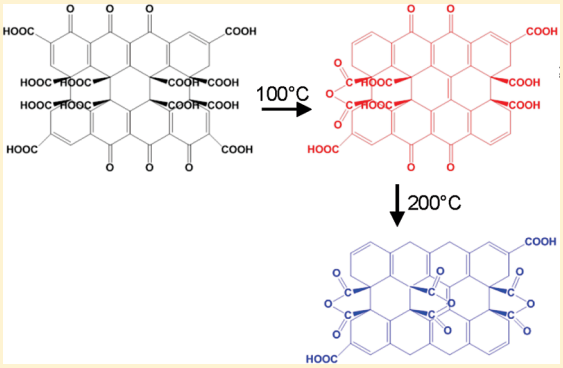

INTRODUCTION

Graphene and its oxidized form graphene oxide (GO) are of significant importance in modern science primarily due to their intrinsic large surface area and excellent electrical, mechanical, and thermal properties. Importantly, these materials have been fabricated and studied for uses in many applications, such as polymer composites, water treatment, energy-related materials, biosensors, field-effect transistors, and biomedical applications. There are numerous methods for the fabrication of graphene including the scotch tape method,[1] liquid phase exfoliation,[2−4] chemical vapor deposition,[5−7] graphitization of silicon carbide,[8] unzipping of carbon nanotubes,[9,10] organic synthesis,[11] and anodic bonding,[12] all of which result in the production of graphene with varying degrees of conductivity.

Chemical functionalization of graphene, to produce GO, typically involves methods in which graphite is oxidized via the Hummer and Offeman,[13] Staudenmaier,[14] or Brodie[15] methods and many variations thereof. All require treatment in aggressive oxidizing agents, often combined with sonication or mechanical and thermal processing. Both the Hummer and Offeman[13] as well as the Staudenmaier methods[14] are known to produce unstable GO with a high degree of contamination and degradation, while GO synthesized using Brodie's method[15] produces a higher quality GO product but still with far lower conductivity than graphene.

While the structure of graphene is well-known, consisting of an atomic layer of carbon atoms arranged in an sp^2 hybridized lattice with either zigzag or armchair edges, the precise chemical structure of GO has been the subject of considerable debate over the years, and even to this day no unambiguous model exists. Nonetheless, GO can be considered as individual sheets of graphene decorated with oxygen functional groups on both the basal planes and edges.[16] Several models have been proposed to elucidate its structure. For example, the Hofmann and Holst[17] model proposed that the graphene basal planes are functionalized with epoxy groups, with a net molecular formula of C_2O, while the Ruess[18] model proposed hydroxyl groups decorated the basal plane. Conversely, Ruess'[18] model altered the basal plane structure to an sp^3 hybridized system, rather than the sp^2 hybridized model, and decorated it with epoxy and hydroxyl functionalities.[18] Ether-like oxygen bridges between the carbon atoms accounted for GO's hydrogen content.[18] This model assumed a repeat unit, where one-quarter of the cyclohexanes contained epoxides at the 1,3-positions with hydroxylation at the 4-position, forming a regular lattice structure.[18] Later Scholz and Boehm replaced the epoxide and ether groups with carbonyl and hydroxyl moieties.[19] Nakajima and Matsuo[20] assumed that two carbon layers linked to each other via sp^3 carbon−carbon bonds perpendicular to the layers with carbonyl and hydroxyl groups present depending on the level of hydration. A commonly accepted model is a mixture of the Ruess[18] and Scholz−Boehm[19] skeleton, including a random distribution of two kinds of domains: that of the trans linked cyclohexane chairs and that of the corrugated hexagon ribbons. This then has varying degrees of oxygenated species, tertiary OH groups and 1,3-ethers lying

Received: June 8, 2013
Revised: September 10, 2013
Published: September 11, 2013

   dx.doi.org/10.1021/jp405682u | J. Phys. Chem. C 2013, 117, 21312−21319

above and below the cyclohexane sheets, while cyclic ketones and quinones can be formed on the hexagon ribbons where the C−C bonds are cleaved.[21]

In order to reinstate GO's conductivity, it is often reduced using thermal reduction, for example, heating GO with *N*,*N*-dimethylacetamide[22] or heating GO using microwave,[23] plasma,[24] electric current,[25] or heated-tip atomic force microscopy.[26] Alternatively, GO may be reduced chemically, for example, using reductants such as hydrazine (N_2H_4),[27,28] alcohol,[29,30] sodium borohydride,[31] hydriodic acid with acetic acid,[32] sodium/potassium hydroxide,[33] aluminum powder,[34] ammonia,[35] hexylamine,[36] sulfur-containing compounds,[37] lysozyme,[38] vitamin C,[39] and poly(norepinephrine).[40] Among these various chemical reducing agents, the most commonly used is hydrazine, which produces highly reduced GO at low temperatures.[27]

As with GO, the structure and electronic properties of rGO are not clearly defined. However, most recently, Park et al.[41] have proposed that hydrazine treatment of GO resulted in pyrazole formation as a result of the reaction between hydrazine and diketones on the GO surface/edges. Hydrazone formation was also proposed from the reaction between hydrazine and ketones.[41] The insertion of an aromatic N_2 moiety in a five-membered ring at the edges is believed to restore the graphitic networks on the basal planes and thus give rise to improved conductivity.[41]

The aim of the present work is to determine how the density of states (DOS) of graphene oxide changes upon heating in vacuum up to 300 °C. We have applied UV photoelectron spectroscopy (UPS) because the UP spectra show directly the DOS. The changes in DOS are related to changes in the chemical nature of GO due to heating or chemical treatment. Thus, the functional groups attached to the graphene backbone of both GO and rGO have to be identified. For determining the changes in the chemical nature, we have employed X-ray photoelectron spectroscopy (XPS) because this technique is both sensitive to the chemical state and is surface sensitive. It is important to apply a surface sensitive technique like XPS for determining the changes in the chemistry of GO because UPS is also a surface sensitive technique. XPS does not necessarily allow one to unambiguously identify the exact nature of functional groups in cases where they are unknown. However, here we use it to identify the class of chemical groups rather than the exact functional group. This is sufficient for correlating the change in DOS to the change in the chemistry of GO. For identifying the class of functional groups, the binding energies of carbon, oxygen, and nitrogen found in XPS are compared with references and those selected which are in agreement with the C6 ring structure of GO. Taking the binding energies of all elements involved into account also enhances the accuracy for identifying the functional groups.

In the following, the XPS data is reported first in order to introduce the change in the chemical state of the GO upon heating. While the focus of our work is on the changes in the DOS derived from the UPS data

EXPERIMENTAL SECTION

Sample Preparation. Highly ordered pyrolytic graphite (HOPG) was purchased from MTI Corporation. GO was purchased from the Graphene Supermarket and used as received. For the production of rGO, GO was reduced using hydrazine monohydrate (Sigma-Aldrich, Australia). GO powder (3 mg) was dispersed in Milli-Q water (18.2 MΩ cm) (1 mL) and ultrasonicated (Unisonics sonicator, FXP10MH) for 1 min to create a colloidal suspension. Hydrazine monohydrate (1 μL) was added to the suspension and the mixture was heated at 80 °C for 12 h with constant stirring using a magnetic stirrer. After cooling to room temperature, the mixture was filtered under vacuum through a Millipore filter (0.45 μm), and the black powder filtrand was then stored in a desiccator for further analysis.

Electron Spectroscopy. HOPG was used as supplied. To create a fresh surface for analysis the top layers were removed using scotch tape. GO and rGO were resuspended in ethanol and a drop of suspension was dried onto silicon substrates. Silicon was used as substrate as it is inert and does not influence the GO. The substrate does not play any further role in the experiments.

Investigations of the samples with XPS, UPS, and MIES were performed in an ultrahigh vacuum (UHV) apparatus built by SPECS (Berlin, Germany). The apparatus was equipped with a two stage cold cathode gas discharge from MFS (Clausthal-Zellerfeld, Germany) to simultaneously generate metastable helium atoms (He* $^3S_1$) and UV light (He I line) and a nonmonochromatic X-ray source for Mg and Al Kα radiation. The spectra of the electrons emitted from the samples were recorded with a hemispherical Phoibos 100 energy analyzer from SPECS. UP and MIE spectra were recorded at a pass energy of 10 eV. At this pass energy, the analyzer has an energy resolution of 400 meV as evaluated from the Fermi edge of polycrystalline silver. High resolution XP spectra were collected using a pass energy of 10 eV for C 1s, O 1s, Na 1s, S 2p, and Si 2p. The angle between the He*/UV light irradiation and the analyzer and the X-ray irradiation and the analyzer are both 54°. The base pressure of the UHV chamber was a few 10^{-10} mbar although UHV conditions are not required for the experiments shown here.

High resolution XP spectra were fitted using combined Gaussian−Lorentzian peaks with background correction using the Shirley method.[42] The fitting procedure used is described in detail in reference.[43]

In a UPS experiment, the sample is irradiated with UV photons leading to photoionization via the photoelectric effect. The energy of emitted electrons is given by

$$E_{\mathrm{kin},h\nu} = E(h\nu) - E_{\mathrm{bin}} \quad (1)$$

where $E_{\mathrm{kin},h\nu}$ is the kinetic energy of the emitted electron, $E(h\nu)$ is the photon energy (21.2 eV for the HeI line used here), and E_{bin} is the binding energy of the electron before excitation. With UPS, the electron density in the near-surface area is measured since the probing depth is limited by the electron mean free path of the emitted electrons. At the excitation energy used in this study, the electron mean free path in organic compounds is around 10−20 Å.[44] For the XPS experiment, an excitation energy of 1253.6 eV (Mg Kα) was used. For XPS, the same relation between kinetic energy of the emitted electrons, excitation energy, and the binding energy holds as for UPS. The methods differ, however, in their probing depth.

MIES is capable of determining the composition of the outermost layer of a sample. MIES uses metastable helium atoms to induce electron emission from a surface, resulting in valence band spectra similar to UPS. Apart from the orbitals in the helium atom, only electron orbitals located in the outermost layer of the sample are involved in the de-excitation process of the metastable helium atoms.[45−47] The sensitivity of MIES exclusively for the outermost layer makes the method

dx.doi.org/10.1021/jp405682u | J. Phys. Chem. C 2013, 117, 21312−21319

useful for probing the functionality of the graphene oxide surface.

RESULTS AND DISCUSSION

Figures 1A and 2 show the C 1s and O 1s XP spectra, respectively, for nonheated GO, GO heated at 100, 200, and 300 °C, and rGO. Figure 1B shows the HOPG spectrum for C 1s. The peak positions are listed in Tables 1−5. The C 1s spectrum of nonheated graphene oxide shows five peaks (Figure 1A). The lack of a major peak around 285 eV implies that almost all the carbon in the sample is oxidized. As a result of this oxidation, there is only a very small peak at 285.1 ± 0.2 eV, attributed to sp^2 hybridized graphite-like carbon atoms.

Three additional peaks at 286.1 ± 0.3, 287.5 ± 0.3, and 289.8 ± 0.2 eV in the C 1s spectrum (Figure 1A) and two peaks at 533.8 ± 0.2 and 535.0 ± 0.2 eV in the O 1s spectrum (Figure 2) can be seen. Given that the sample is GO, these peaks have to be interpreted as a C6 ring network with oxidized functional groups. A likely interpretation is to attribute the peaks to a mixture of carboxyl groups bound to the C6 network and benzoquinone type species. This interpretation of the XPS data is justified as there must be a C6 ring network and highly oxidized carbon. In fact, examples can be found in literature that show very similar peaks in XP spectra. Barth et al.[48] have shown that pyromellitic acid shows no C peak at 285 eV but two carbon peaks around 286 and 290 eV and two oxygen peaks at 533 and 534.3 eV. These closely match those found in this work. It must be noted that in pyromellitic acid four carboxyl groups are bound to the C6 ring and thus all carbon atoms are affected by the presence of the carboxyl groups. Otha et al.[49] found that the carbonyl group in benzoquinone showed a peak similar to that observed at 287.5 ± 0.3 eV in the nonheated GO sample (Figure 1A; Table 1). They also suggested that a peak should be observed at approximately 532.5 eV in the O 1s spectrum;[49] however, due to the peak at 533.8 ± 0.2 eV (Figure 2) being very broad, it is likely that this peak is concealed and therefore could not be fitted to this binding energy. It can be seen from Table 1 that the assignment of the C and O peaks is supported by the peak intensities found. In summary, the nonheated GO consists almost exclusively of carbon that has formed a bond to either a carboxyl group or a carbonyl group. Such a configuration may be more appropriately described as a Scholz-Boehm type model[19] in which the hydroxyl groups have been more highly oxidized to carboxyl groups.

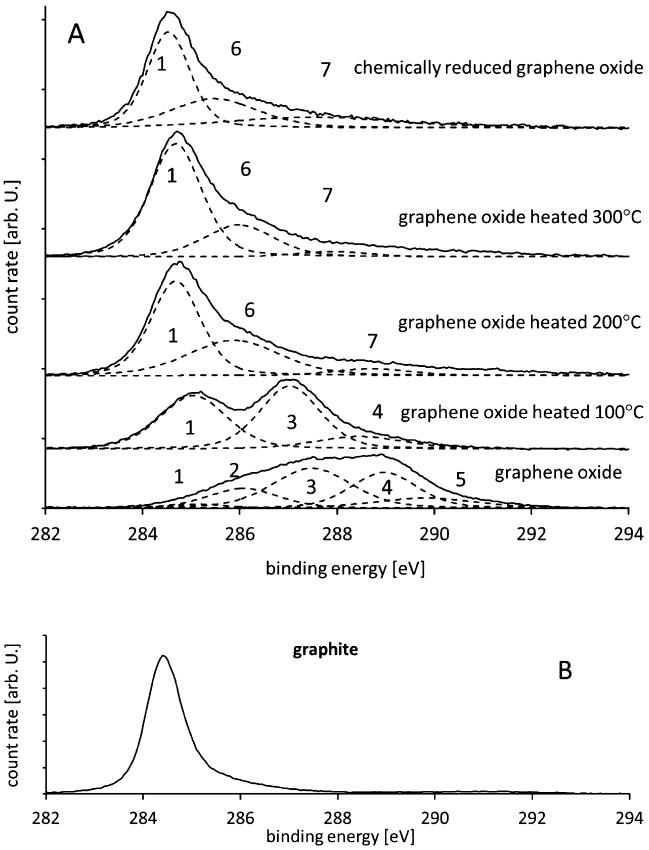

Figure 1. (A) C 1s spectra of nonheated GO at room temperature and heated up to 300 °C and chemically rGO. Assignments of the peaks are given in Tables 1−5. (B) C 1s spectrum of HOPG.

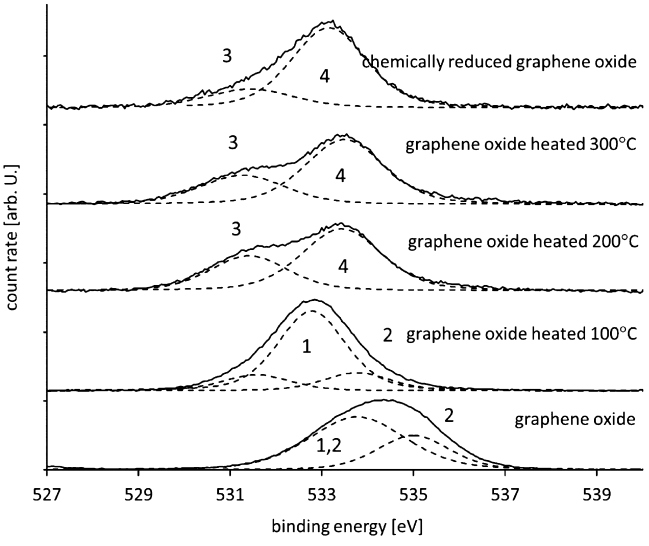

Figure 2. O 1s spectra of nonheated GO at room temperature and heated up to 300 °C and chemically rGO. Assignments of the peaks are given in Tables 1−5.

Table 1. Position, Intensity, and Chemical Nature of the Peaks in the XP Spectra of Non-Heated Graphene Oxide

peak	peak position [eV]	intensity [%]	chemical group
C 1s (1)	285.1 ± 0.2	2 ± 1	sp^2 hybridized graphite-like carbon
C 1s (2)	286.1 ± 0.3	9 ± 1	$C_6H_x(COOH)_{6-x}$, C not bound to carboxyl[48]
C 1s (3)	287.5 ± 0.3	21 ± 1	C in ring bound to O,[49] benzoquinone type
C 1s (4)	289.0 ± 0.2	19 ± 1	$C_6H_x(COOH)_{6-x}$, C bound to carboxyl[48]
C 1s (5)	289.8 ± 0.2	5 ± 1	multiple C6 rings[56]
Na 1s	1072.5 ± 0.3	2 ± 0.5	
S 2p 3/2	169.5 ± 0.3	2 ± 0.5	
O 1s (1,2)	533.8 ± 0.2	25 ± 1	(a) $C_6H_x(COOH)_{6-x}$, O in double bond,[48] (b) benzoquinone $C_6H_4O_2$[49]
O 1s (2)	535.0 ± 0.2	12 ± 1	$C_6H_x(COOH)_{6-x}$, O in single bond[48]
Si 2p 3/2	103.1 ± 0.4	1 ± 0.5	Si in SiO_2
Si 2p 3/2	99.8 ± 0.2	0.5 ± 0.5	Si

dx.doi.org/10.1021/jp405682u | J. Phys. Chem. C 2013, 117, 21312−21319

Further in the O 1s spectrum, a very small Si−O peak can be seen from the substrate and a small amount of sulfur and sodium which can be attributed to Na_2SO_4.[50] This is most likely present as a result of acid neutralization after the oxidation process in the formation of the GO.

The UP spectra of nonheated GO at room temperature and heated up to 300 °C and chemically rGO are shown in Figure 3A. The various states formed in the valence electron region are shown according to Luo et al.[51] In the valence electron region, oxygen (O 2p) can be found between 5 and 7.5 eV.[45,52] Oxygen due to −OH and −COOH can be found at somewhat higher binding energy.[45,52] Of interest for the present study is the $2p\pi$ region of graphene at very low binding energies and the O 2p region which is partially overlapping with the $2p\sigma$ of the GO. The low binding energy region is shown separately in Figure 3B. The nonheated GO shows a very low DOS in the $2p\pi$ region due to the fact that all the carbon is highly oxidized, as can be seen in the XP spectra.

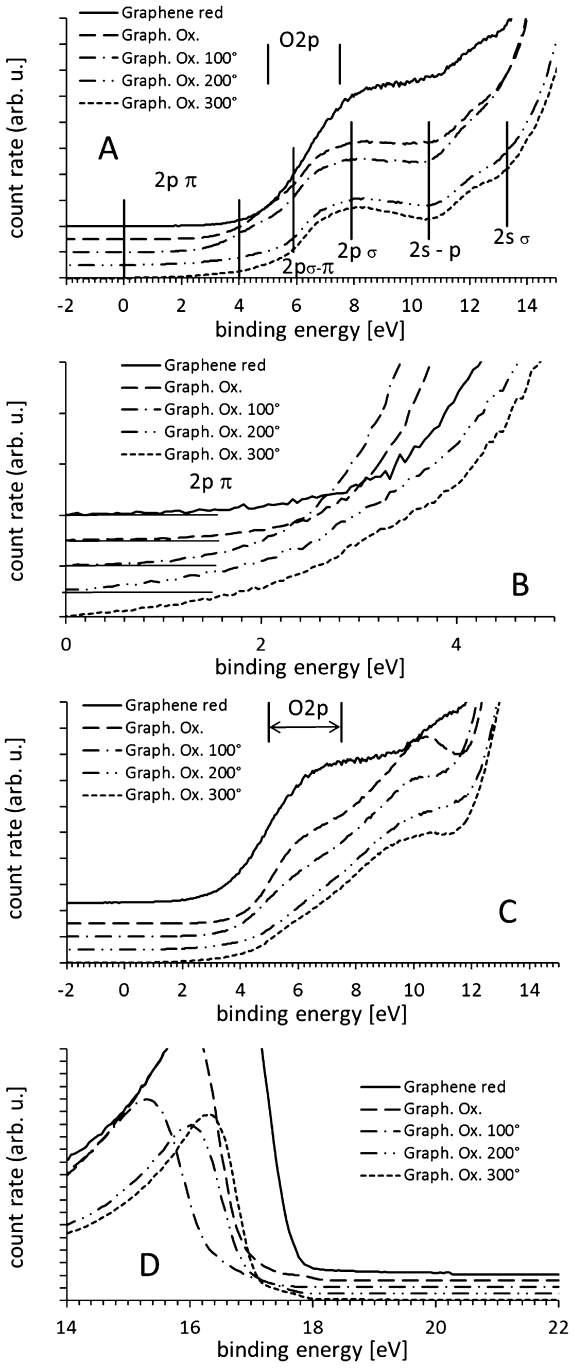

Figure 3. (A) UP spectra of nonheated GO at room temperature and heated up to 300 °C and chemically rGO. The assignment of the regions is according to Luo et al.[51] for graphene and Voigts et al.[57] for oxygen. (B) Low binding energy region illustrating the change of the density of states in the 2 p π region. (C) MIE spectra of GO and GO heated up to 300 °C as well as the and chemically rGO. (D) Secondary electron cutoff of the UP spectra used to determine the work function.

The MIE spectra of GO and GO heated to 100 °C are shown in Figure 3C. In the figure, the O 2p region is highlighted as this is of main interest here. The other regions are similar to those assigned in the UP spectrum. However, the de-excitation mechanism of the metastable helium atom for the carbon related structures could change from resonant ionization (RI) followed by Auger-neutralization (AN) to Auger-de-excitation in case the DOS close to the Fermi level increase significantly.[46] Unambiguous assignment of the carbon regions in the MIE spectrum is thus more difficult. However, a contribution of O 2p can clearly be identified.

The secondary electron cutoff of the UP spectra is shown in Figure 3C. The cutoff can be used to determine the work function of the sample, which is 4.2 ± 0.1 eV for the nonheated GO sample.

The XP spectrum of GO heated to 100 °C shows a peak at 285.0 ± 0.2, 287.0 ± 0.3, and 288.5 ± 0.3 eV in the C 1s spectrum (Figure 1A). Oxygen is found at 531.6 ± 0.4, 532.8 ± 0.2, and 533.8 ± 0.2 eV (Figure 2). The combination of these peaks can again be assigned to a mixture of carboxyl groups bound to the C6 network and benzoquinone type species. The C 1s spectrum shows that the fraction of carboxyl groups decreases upon heating to 100 °C which also leads to the appearance of the carbon bonded to carbon peak at 285 eV. The appearance of the peak at 285 eV could also be considered to arise from a shift in the 286 eV peak. A similar change in the C 1s spectrum was observed by Barth et al.[48] when reducing the number of carboxyl groups attached to the C6 ring, that is, during the transition from pyromellitic acid to phthalic acid. This transition can be attributed to the fact that in phthalic acid not all carbon atoms of the C6 ring are affected by the presence of the carboxylic groups. Barth et al.[48] found that at the same time the O 1s peak also moves to a lower binding energy for approximately 0.5 to 0.6 eV. In our case, the O 1s peak moves for approximately 1 eV, leading to peaks at 533.8 ± 0.2 and 532.8 ± 0.2 eV (Figure 2). The C 1s peak at 287.0 ± 0.3 eV (Figure 1A) is attributed to benzoquinone type species as well as a fraction of the O 1s peak at 532.8 ± 0.2 and 533.8 ± 0.2 eV (Figure 2). It should be noted that the O 1s spectrum of the GO heated to 100 °C is very broad and that it is hard to fit peaks unambiguously. A separate O 1s peak at 531.6 ± 0.4 eV may arise from oxygen in carboxyl groups or benzoquinone-type species (Figure 2). However, it might also be part of a carbonyl related to dianhydrides that appears at higher heating temperatures. It can be seen from Table 2 that the assignment of the C and O peaks is supported by the peak intensities found.

For comparison, the C 1s XP spectrum of HOPG is shown in Figure 1B. Graphite shows a single peak at 284.4 eV and weak intensities around 290 eV which are attributed to $\pi \rightarrow \pi^*$ transitions.[53] These are not observed to any meaningful extent in the GO or rGO samples.

dx.doi.org/10.1021/jp405682u | J. Phys. Chem. C 2013, 117, 21312−21319

Table 2. Position, Intensity, and Chemical Nature of the Peaks in the XP Spectra of Graphene Oxide Heated to 100 °C

peak	peak position [eV]	intensity [%]	chemical group
C 1s (1)	285.0 ± 0.2	24 ± 1	sp^2 hybridized graphite-like carbon
C 1s (2)	286.1 ± 0.3	0 ± 1	$C_6H_x(COOH)_{6-x}$, C not bound to carboxyl[48]
C 1s (3)	287.0 ± 0.3	25 ± 1	C in ring bound to O[49] (benzoquinone type)
C 1s (4)	288.5 ± 0.3	7 ± 1	$C_6H_x(COOH)_{6-x}$, C bound to carboxyl[48]
Na 1s	107.6 ± 0.3	2 ± 0.5	
S 2p 3/2	168.3 ± 0.3	2 ± 0.5	
O 1s (1)	531.6 ± 0.4	5 ± 1	O bound to C6 ring,[49] (benzoquinone type)
O 1s (1)	532.8 ± 0.2	26 ± 1	(a) $C_6H_x(COOH)_{6-x}$, O in double bond[48], (b) benzoquinone $C_6H_4O_2$[49]
O 1s (2)	533.8 ± 0.2	6 ± 1	$C_6H_x(COOH)_{6-x}$, O in single bond[48]
Si 2p 3/2	99.8 ± 0.2	1 ± 0.5	Si
Si 2p 3/2	103.3 ± 0.4	0.5 ± 0.5	Si in SiO_2

The UP spectra of the GO heated to 100 °C is similar to the nonheated GO sample (see Figure 3A). However, in the low binding energy region, shown in Figure 3B, the DOS increases slightly compared to the nonheated GO sample. The increase is most likely a consequence of the removal of the carboxyl groups and partial restoration of the C6 graphene network. In the O 2p region, no significant change in the spectrum can be seen.

The MIE spectra in Figure 3C show a decrease in the O 2p region. Due to the sensitivity of MIES for exclusively the outermost layer, it can be concluded that the decrease of the benzoquinone species is stronger at the outermost layer than in deeper layers. The work function of the GO heated to 100 °C has now increased from 4.2 ± 0.1 eV for the nonheated GO sample to 4.8 ± 0.1 eV. The reason for the increase in work function is probably the decrease in carboxyl groups which could lead to a less symmetric distribution of the carboxyl group. The carboxyl group causes a polarization of the molecule. In the nonheated sample, the carboxyl groups are most likely distributed symmetrically relative to the C6 rings while cleaving a fraction of the carboxyl groups could lead to a less symmetric distribution and cause an increase in the work function. A change in the work function of GO due to the change of the number of functional groups was proposed by Kumar et al. who have carried out molecular dynamics calculations.[54] Kumar et al., however, attributed the high work function of GO to the presence of carbonyl groups and not, as we propose here, to an asymmetric distribution of such groups relative to the surface plane.

The GO heated to 200 °C shows a qualitative change in the functional groups and DOS compared to the sample heated to 100 °C (Figure 1A). These changes are attributed to a reaction in the GO upon heating from 100 to 200 °C. The C 1s peak at 285 eV associated with the sp^2 hybridized graphite-like carbon atoms has increased in intensity and shifted to 284.7 ± 0.3 eV. A new peak appears at 285.9 ± 0.3 eV, while a small peak at 288.0 ± 0.5 eV is also observed. The O 1s XP spectrum shows a major peak at 533.4 ± 0.2 eV and a smaller peak at 531.4 ± 0.2 eV. The C 1s peak at 285.9 ± 0.3 eV and the oxygen peak at 533.4 ± 0.2 eV can be assigned to C−O−C ether-like structures associated with dianhydrides while the C 1s peak at 288.0 ± 0.5 eV and the O 1s peak at 531.4 ± 0.2 eV can be assigned to a ketone like structures of anhydrides.[55] Of the anhydride π-conjugated organic molecules investigated in ref 55, the 1,4,5,8-naphthalene-tetracarboxylic acid dianhydride comes closest to the structure proposed here. It must be noted that the C 1s peak at 288 eV has a large uncertainty in intensity and position, partially because it is difficult to distinguish from the $\pi \rightarrow \pi^*$ transitions. It can be seen from Table 3 that the assignment of the C and O peaks is supported by the peak intensities found.

Table 3. Position, Intensity, and Chemical Nature of the Peaks in the XP Spectra of Graphene Oxide Heated to 200°C

peak	peak position [eV]	intensity [%]	chemical group
C 1s (1)	284.7 ± 0.2	43 ± 1	C−C
C 1s (6)	285.9 ± 0.3	19 ± 1	ether involving 2 C6 rings[55]
C 1s (7)	288.0 ± 0.5	7 ± 1	ketone[55]
Na 1s	1071.8 ± 0.3	2 ± 0.5	
S 2p 3/2	168.1 ± 0.3	2 ± 0.5	
O 1s (3)	531.4 ± 0.2	9 ± 1	ketone[55]
O 1s (4)	533.4 ± 0.2	16 ± 1	ether involving 2 C6 rings[55]
Si 2p 3/2	99.8 ± 0.2	2 ± 0.5	Si
Si 2p 3/2	103.3 ± 0.4	0.5 ± 0.5	Si in SiO_2

The UP spectra of the GO heated to 200 °C is quite different from those of the nonheated GO and GO heated to 100 °C samples (see Figure 3A). In the low binding energy region, shown in Figure 3B, the DOS of the GO heated to 200 °C increases considerably compared to the 100 °C heated sample. In the O 2p region no significant change in the shape of the spectrum can be seen. The increase in intensity seems to be partially attributed to the increase in the 2pπ region. In the XP spectra we saw that the total oxygen intensity decreases from 37% to 25%. However, the nature of the oxygen compounds changes from carboxylic and benzoquinone type to dianhydride type. The latter have the character of O 2p species and should be found in the 5 to 7.5 eV region. Thus, the increase in intensity in the O 2p region might also be due to the increase in 2p intensity. In the MIE spectrum, the intensity is decreasing in the O 2p. Thus the oxygen species attributed to the O 2p region decrease stronger in the outermost layer compared to the inner graphene sheets. This implies that it is easier to remove the oxygen species from the outermost layer as they do not have to travel through a number of graphene sheets.

The work function of the GO heated to 200 °C returns to that of the nonheated GO sample, namely 4.2 ± 0.1 eV. The reason for the decrease in work function back to the value of the nonheated sample could be that the oxidiized functional groups are removed. This interpretation is supported by XPS which shows that the peak between 288.5 to 289 eV disappears when heating the sample to 200 °C and subsequently to 300 °C. The high work function of the sample heated to 100 °C was interpreted as asymmetric electron density distribution relative to the surface plane caused by a partial removal of the carboxyl or carbonyl group. With the removal of these functional groups, the electron density at the outermost layer becomes again more symmetric and causes a decrease in the work function.

The XP spectra of the GO heated to 300 °C are very similar to those of the GO heated to 200 °C (Figures 1A and 2; Table

dx.doi.org/10.1021/jp405682u | J. Phys. Chem. C 2013, 117, 21312−21319

4). The position of the C 1s and O 1s peaks are the same in both samples while the intensity of the 285 eV peak has slightly

Table 4. Position, Intensity, and Chemical Nature of the Peaks in the XP Spectra of Graphene Oxide Heated to 300°C

peak	peak position [eV]	intensity [%]	chemical group
C 1s (1)	284.7 ± 0.2	50 ± 1	sp^2 hybridized graphite-like carbon
C 1s (6)	286.0 ± 0.3	19 ± 1	C−O−C in dianhydrides involving 2 C6 rings[55]
C 1s (7)	287.9 ± 0.5	3 ± 1	ketone[55]
Na 1s	1072.0 ± 0.3	2 ± 0.5	
S 2p 3/2	168.2 ± 0.3	1 ± 0.5	
O 1s (3)	531.3 ± 0.2	7 ± 1	ketone[55]
O 1s (4)	533.5 ± 0.2	15 ± 1	C−O−C in dianhydrides involving 2 C6 rings[55]
Si 2p 3/2	99.9 ± 0.2	2 ± 0.5	Si
Si 2p 3/2	103.5 ± 0.4	0.5 ± 0.5	Si in SiO_2

increased and all other C 1s and O 1s peaks have decreased. In addition, the UP spectra are almost identical (Figure 3A and B). In the MIE spectra the O 2p intensity decreases implying again that it is easier to remove the oxygen related groups from the surface compared to the deeper lying graphene sheets (Figure 3C). Furthermore the work function is the same as in the nonheated GO and GO heated to 200 °C samples, namely, 4.2 ± 0.1 eV.

Figure 4 shows the proposed structure of GO and after heating to 100 °C then to 200 °C then to 300 °C. This highlights the transformation of a highly oxygenated sheets consisting of carboxyl and benzoquinone moieties to dianhydrides and finally with very little oxygenation.

The XP spectra of the chemically reduced graphene oxide sample are very similar to those of the GO heated to 200 and 300 °C (Figures 1A (C 1s) and 2 (O 1s), and Table 5). The only difference is that the sp^2 hybridized graphite-like carbon has decreased, the C 1s peak at 287.5 ± 0.5 eV has increased and that nitrogen now appears in the XP spectrum at a binding energy of 399.8 ± 0.4 eV. The combination of a carbon peak at 287.5 eV and a nitrogen peak at 399.8 eV is typical for an pyrazolidine species[41] and is a consequence of the hydrazine treatment. The nitrogen peak is very broad with a full-width-half-maximum (fwhm) of 3.5 eV and has to be considered to cover both nitrogen−carbon bonds species in the pyrazolidine species or pyrazole peak, as suggested by Park et al.[41] The UP spectrum shows low DOS at low binding energies. Thus the formation of the nitrogen carbon bond is interrupting the $2p\pi$ structure in the graphene and the work function has decreased to 3.4 eV. This confirms previous reports by Park et al[41] who

Table 5. Position, Intensity, and Chemical Nature of the Peaks in the XP Spectra of Chemically Reduced Graphene Oxide

peak	peak position [eV]	intensity [%]	chemical group
C 1s (1)	284.5 ± 0.2	30 ± 1	sp^2 hybridized graphite-like carbon
C 1s (6)	285.5 ± 0.3	19 ± 1	C−O−C in dianhydrides involving 2 C6 rings[55]
C 1s (7)	287.5 ± 0.5	13 ± 1	ketone[55]
Na 1s	1071.4 ± 0.3	0.9 ± 0.2	
S 2p 3/2	163.9 ± 0.3	2.3 ± 0.5	
O 1s (3)	531.4 ± 0.3	5 ± 1	ketone[55]
O 1s (4)	533.0 ± 0.2	18 ± 1	C−O−C in dianhydrides involving 2 C6 rings[55]
N 1s	399.8 ± 0.4	3 ± 1	pyrazolidine[41]
Si 2p 3/2	99.9 ± 0.2	6 ± 1	Si
Si 2p 3/2	103.5 ± 0.4	1.5 ± 1	Si in SiO_2

suggest the formation of pyrazole rings at vicinal C═O groups at the edges of GO which has been reduced with hydrazine.

CONCLUSIONS

Here we show that as-purchased GO contains predominately carboxyl and benzoquinone-type functional groups which have removed all density of states in the $2p\pi$ region. Heating this GO to 100 °C is sufficient to remove a fraction of the carboxyl groups and restore some of the $2p\pi$ DOS. Further, it is proposed that adjacent carboxyl groups undergo a condensation reaction to form dianhydrides. Heating to 200 °C removes the benzoquinone-type functionalities and appears to restore the $2p\pi$ DOS, as shown with UPS. Heating the GO further 300 °C does not lead to any significant change in the samples. Removal of oxygen based functional groups through heat treatment is more successful for the outermost GO layer, as shown by MIES. Chemical reduction using hydrazine successfully removes the oxygen based functional groups and introduces pyrazolidine or pyrazole groups into the network which does not lead to the restoration of the $2p\pi$ DOS.

AUTHOR INFORMATION

Notes

The authors declare no competing financial interest.

ACKNOWLEDGMENTS

We acknowledge Flinders University for financial support. The work was also supported by a grant of the Australian Research Council (LE0989068).

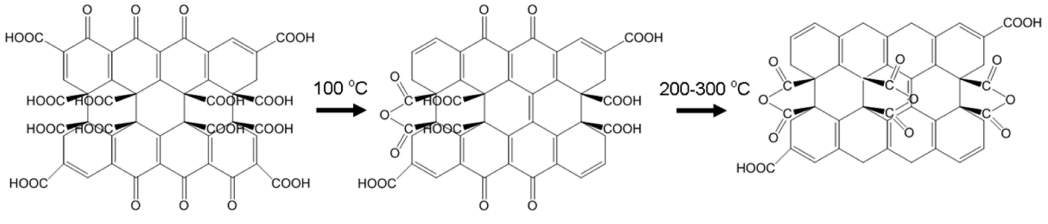

Figure 4. Proposed structures of, from left to right, nonheated GO, GO heated to 100 °C, and GO heated to 200 and 300 °C.

dx.doi.org/10.1021/jp405682u | J. Phys. Chem. C 2013, 117, 21312−21319

REFERENCES

(1) Novoselov, K. S.; Geim, A. K.; Morozov, S. V.; Jiang, D.; Zhang, Y.; Dubonos, S. V.; Grigorieva, I. V.; Firsov, A. A. Electric Field Effect in Atomically Thin Carbon Films. *Science* **2004**, *306*, 666−669.

(2) Hernandez, Y.; Nicolosi, V.; Lotya, M.; Blighe, F. M.; Sun, Z.; De, S.; McGovern, I. T.; Holland, B.; Byrne, M.; Gun'Ko, Y. K.; et al. High-Yield Production of Graphene by Liquid-Phase Exfoliation of Graphite. *Nat. Nano* **2008**, *3*, 563−568.

(3) Lotya, M.; Hernandez, Y.; King, P. J.; Smith, R. J.; Nicolosi, V.; Karlsson, L. S.; Blighe, F. M.; De, S.; Wang, Z.; McGovern, I. T.; et al. Liquid Phase Production of Graphene by Exfoliation of Graphite in Surfactant/Water Solutions. *J. Am. Chem. Soc.* **2009**, *131*, 3611−3620.

(4) Mukherjee, A.; Kang, J.; Kuznetsov, O.; Sun, Y.; Thaner, R.; Bratt, A. S.; Lomeda, J. R.; Kelly, K. F.; Billups, W. E. Water-Soluble Graphite Nanoplatelets Formed by Oleum Exfoliation of Graphite. *Chem. Mater.* **2010**, *23*, 9−13.

(5) Bae, S.; Kim, H.; Lee, Y.; Xu, X.; Park, J.-S.; Zheng, Y.; Balakrishnan, J.; Lei, T.; Ri Kim, H.; Song, Y. I.; et al. Roll-to-Roll Production of 30-Inch Graphene Films for Transparent Electrodes. *Nat. Nano* **2010**, *5*, 574−578.

(6) Reina, A.; Jia, X.; Ho, J.; Nezich, D.; Son, H.; Bulovic, V.; Dresselhaus, M. S.; Kong, J. Large Area, Few-Layer Graphene Films on Arbitrary Substrates by Chemical Vapor Deposition. *Nano Lett.* **2008**, *9*, 30−35.

(7) Zhu, Y.; Murali, S.; Stoller, M. D.; Ganesh, K. J.; Cai, W.; Ferreira, P. J.; Pirkle, A.; Wallace, R. M.; Cychosz, K. A.; Thommes, M.; et al. Carbon-Based Supercapacitors Produced by Activation of Graphene. *Science* **2011**, *332*, 1537−1541.

(8) Emtsev, K. V.; Bostwick, A.; Horn, K.; Jobst, J.; Kellogg, G. L.; Ley, L.; McChesney, J. L.; Ohta, T.; Reshanov, S. A.; Rohrl, J.; et al. Towards Wafer-Size Graphene Layers by Atmospheric Pressure Graphitization of Silicon Carbide. *Nat. Mater.* **2009**, *8*, 203−207.

(9) Jiao, L.; Zhang, L.; Wang, X.; Diankov, G.; Dai, H. Narrow Graphene Nanoribbons from Carbon Nanotubes. *Nature* **2009**, *458*, 877−880.

(10) Vogt, A. P.; Gibson, C. T.; Tune, D. D.; Bissett, M. A.; Voelcker, N. H.; Shapter, J. G.; Ellis, A. V. High-Order Graphene Oxide Nanoarchitectures. *Nanoscale* **2011**, *3*, 3076−3079.

(11) Qian, H.; Negri, F.; Wang, C.; Wang, Z. Fully Conjugated Tri(Perylene Bisimides): An Approach to the Construction of N-Type Graphene Nanoribbons. *J. Am. Chem. Soc.* **2008**, *130*, 17970−17976.

(12) Moldt, T.; Eckmann, A.; Klar, P.; Morozov, S. V.; Zhukov, A. A.; Novoselov, K. S.; Casiraghi, C. High-Yield Production and Transfer of Graphene Flakes Obtained by Anodic Bonding. *ACS Nano* **2011**, *5*, 7700−7706.

(13) Hummers, W. S.; Offeman, R. E. Preparation of Graphitic Oxide. *J. Am. Chem. Soc.* **1958**, *80*, 1339−1339.

(14) Staudenmaier, L. Verfahren Zur Darstellung Der Graphitsäure. *Ber. Dtsch. Chem. Ges.* **1898**, *31*, 1481−1487.

(15) Brodie, B. C. On the Atomic Weight of Graphite. *Philos. Trans. R. Soc. London* **1859**, *149*, 249−259.

(16) Saxena, S.; Tyson, T. A.; Shukla, S.; Negusse, E.; Chen, H.; Bai, J. Investigation of Structural and Electronic Properties of Graphene Oxide. *Appl. Phys. Lett.* **2011**, *99*, 013104−3.

(17) Hofmann, U.; Holst, R. Über Die Säurenatur Und Die Methylierung Von Graphitoxyd. *Ber. Dtsch. Chem. Ges.* **1939**, *72*, 754−771.

(18) Ruess, G. Über Das Graphitoxyhydroxyd (Graphitoxyd). *Monatsh. Chem.* **1947**, *76*, 381−417.

(19) Scholz, W.; Boehm, H. P. Untersuchungen Am Graphitoxid. Vi. Betrachtungen Zur Struktur Des Graphitoxids. *Z. Anorg. Allg. Chem.* **1969**, *369*, 327−340.

(20) Nakajima, T.; Matsuo, Y. Formation Process and Structure of Graphite Oxide. *Carbon* **1994**, *32*, 469−475.

(21) Szabó, T.; Berkesi, O.; Forgó, P.; Josepovits, K.; Sanakis, Y.; Petridis, D.; Dékány, I. Evolution of Surface Functional Groups in a Series of Progressively Oxidized Graphite Oxides. *Chem. Mater.* **2006**, *18*, 2740−2749.

(22) Chen, W.; Yan, L. Preparation of Graphene by a Low-Temperature Thermal Reduction at Atmosphere Pressure. *Nanoscale* **2010**, *2*, 559−563.

(23) Chen, W.; Yan, L.; Bangal, P. R. Preparation of Graphene by the Rapid and Mild Thermal Reduction of Graphene Oxide Induced by Microwaves. *Carbon* **2010**, *48*, 1146−1152.

(24) Baraket, M.; Walton, S. G.; Wei, Z.; Lock, E. H.; Robinson, J. T.; Sheehan, P. Reduction of Graphene Oxide by Electron Beam Generated Plasmas Produced in Methane/Argon Mixtures. *Carbon* **2010**, *48*, 3382−3390.

(25) Yao, P.; Chen, P.; Jiang, L.; Zhao, H.; Zhu, H.; Zhou, D.; Hu, W.; Han, B.-H.; Liu, M. Electric Current Induced Reduction of Graphene Oxide and Its Application as Gap Electrodes in Organic Photoswitching Devices. *Adv. Mater.* **2010**, *22*, 5008−5012.

(26) Wei, Z.; Wang, D.; Kim, S.; Kim, S.-Y.; Hu, Y.; Yakes, M. K.; Laracuente, A. R.; Dai, Z.; Marder, S. R.; Berger, C.; et al. Nanoscale Tunable Reduction of Graphene Oxide for Graphene Electronics. *Science* **2010**, *328*, 1373−1376.

(27) Stankovich, S.; Dikin, D. A.; Piner, R. D.; Kohlhaas, K. A.; Kleinhammes, A.; Jia, Y.; Wu, Y.; Nguyen, S. T.; Ruoff, R. S. Synthesis of Graphene-Based Nanosheets Via Chemical Reduction of Exfoliated Graphite Oxide. *Carbon* **2007**, *45*, 1558−1565.

(28) Wang, H.; Robinson, J. T.; Li, X.; Dai, H. Solvothermal Reduction of Chemically Exfoliated Graphene Sheets. *J. Am. Chem. Soc.* **2009**, *131*, 9910−9911.

(29) Dreyer, D. R.; Murali, S.; Zhu, Y.; Ruoff, R. S.; Bielawski, C. W. Reduction of Graphite Oxide Using Alcohols. *J. Mater. Chem.* **2011**, *21*, 3443−3447.

(30) Su, C.-Y.; Xu, Y.; Zhang, W.; Zhao, J.; Liu, A.; Tang, X.; Tsai, C.-H.; Huang, Y.; Li, L.-J. Highly Efficient Restoration of Graphitic Structure in Graphene Oxide Using Alcohol Vapors. *ACS Nano* **2010**, *4*, 5285−5292.

(31) Shin, H.-J.; Kim, K. K.; Benayad, A.; Yoon, S.-M.; Park, H. K.; Jung, I.-S.; Jin, M. H.; Jeong, H.-K.; Kim, J. M.; Choi, J.-Y.; et al. Efficient Reduction of Graphite Oxide by Sodium Borohydride and Its Effect on Electrical Conductance. *Adv. Funct. Mater.* **2009**, *19*, 1987−1992.

(32) Moon, I. K.; Lee, J.; Ruoff, R. S.; Lee, H. Reduced Graphene Oxide by Chemical Graphitization. *Nat. Commun.* **2010**, *1*, 73.

(33) Fan, X.; Peng, W.; Li, Y.; Li, X.; Wang, S.; Zhang, G.; Zhang, F. Deoxygenation of Exfoliated Graphite Oxide under Alkaline Conditions: A Green Route to Graphene Preparation. *Adv. Mater.* **2008**, *20*, 4490−4493.

(34) Fan, Z.; Wang, K.; Wei, T.; Yan, J.; Song, L.; Shao, B. An Environmentally Friendly and Efficient Route for the Reduction of Graphene Oxide by Aluminum Powder. *Carbon* **2010**, *48*, 1686−1689.

(35) Li, X.; Wang, H.; Robinson, J. T.; Sanchez, H.; Diankov, G.; Dai, H. Simultaneous Nitrogen Doping and Reduction of Graphene Oxide. *J. Am. Chem. Soc.* **2009**, *131*, 15939−15944.

(36) Compton, O. C.; Dikin, D. A.; Putz, K. W.; Brinson, L. C.; Nguyen, S. T. Electrically Conductive "Alkylated" Graphene Paper Via Chemical Reduction of Amine-Functionalized Graphene Oxide Paper. *Adv. Mater.* **2010**, *22*, 892−896.

(37) Zhou, T.; Chen, F.; Liu, K.; Deng, H.; Zhang, Q.; Feng, J.; Fu, Q. A Simple and Efficient Method to Prepare Graphene by Reduction of Graphite Oxide with Sodium Hydrosulfite. *Nanotechnology* **2011**, *22*, 045704.

(38) Yang, F.; Liu, Y.; Gao, L.; Sun, J. Ph-Sensitive Highly Dispersed Reduced Graphene Oxide Solution Using Lysozyme Via an in Situ Reduction Method. *J. Phys. Chem. C* **2010**, *114*, 22085−22091.

(39) Fernández-Merino, M. J.; Guardia, L.; Paredes, J. I.; Villar-Rodil, S.; Solís-Fernández, P.; Martínez-Alonso, A.; Tascón, J. M. D. Vitamin C Is an Ideal Substitute for Hydrazine in the Reduction of Graphene Oxide Suspensions. *J. Phys. Chem. C* **2010**, *114*, 6426−6432.

(40) Kang, S. M.; Park, S.; Kim, D.; Park, S. Y.; Ruoff, R. S.; Lee, H. Simultaneous Reduction and Surface Functionalization of Graphene Oxide by Mussel-Inspired Chemistry. *Adv. Funct. Mater.* **2011**, *21*, 108−112.

(41) Park, S.; Hu, Y.; Hwang, J. O.; Lee, E.-S.; Casabianca, L. B.; Cai, W.; Potts, J. R.; Ha, H.-W.; Chen, S.; Oh, J.; et al. Chemical Structures of Hydrazine-Treated Graphene Oxide and Generation of Aromatic Nitrogen Doping. *Nat. Commun.* **2012**, *3*, 638.
(42) Shirley, D. A. High-Resolution X-Ray Photoemission Spectrum of the Valence Bands of Gold. *Phys. Rev. B: Condens. Matter* **1972**, *5*, 4709−4714.
(43) Anderson, D. P.; Alvino, J. F.; Gentleman, A.; Qahtani, H. A.; Thomsen, L.; Polson, M. I. J.; Metha, G. F.; Golovko, V. B.; Andersson, G. G. Chemically-Synthesised, Atomically-Precise Gold Clusters Deposited and Activated on Titania. *Phys. Chem. Chem. Phys.* **2013**, *15*, 3917−3929.
(44) Seah, M. P.; Dench, W. A. Quantitative Electron Spectroscopy of Surfaces: A Standard Data Base for Electron Inelastic Mean Free Paths in Solids. *Surf. Interface Anal.* **1979**, *1*, 2−11.
(45) Krischok, S.; Günster, J.; Goodman, D. W.; Höfft, O.; Kempter, V. Mies and Ups(Hei) Studies on Reduced Tio_2(110). *Surf. Interface Anal.* **2005**, *37*, 77−82.
(46) Morgner, H. The Characterization of Liquid and Solid Surfaces with Metastable Helium Atoms. In *Advances in Atomic, Molecular, and Optical Physics*; Benjamin, B., Herbert, W., Eds.; Academic Press: San Diego, CA, 2000; Vol. *42*, pp 387−488.
(47) Oberbrodhage, J. The Behaviour of Phase Transfer Catalysts in Polar Solvents: A Mies Study of Onium Salts in Formamide. *J. Electron Spectrosc. Relat. Phenom.* **1998**, *95*, 171−191.
(48) Barth, G.; Linder, R.; Bryson, C. Advances in Charge Neutralization for Xps Measurements of Nonconducting Materials. *Surf. Interface Anal.* **1988**, *11*, 307−311.
(49) Ohta, T.; Yamada, M.; Kuroda, H. X-Ray Photoelectron Spectroscopy of *P*-Benzoquinone, Hydroquinone and Their Halogen-Substituted Derivatives. *Bull. Chem. Soc. Jpn.* **1974**, *47*, 1158−1161.
(50) Turner, N. H.; Murday, J. S.; Ramaker, D. E. Quantitative Determination of Surface Composition of Sulfur Bearing Anion Mixtures by Auger Electron Spectroscopy. *Anal. Chem.* **1980**, *52*, 84−92.
(51) Luo, Z.; Lim, S.; Tian, Z.; Shang, J.; Lai, L.; MacDonald, B.; Fu, C.; Shen, Z.; Yu, T.; Lin, J. Pyridinic N Doped Graphene: Synthesis, Electronic Structure, and Electrocatalytic Property. *J. Mater. Chem.* **2011**, *21*, 8038−8044.
(52) Voigts, F.; Argirusis, C.; Maus-Friedrichs, W. The Interaction of H_2o with Fe-Doped $Srtio_3$(100) Surfaces. *Surf. Interface Anal.* **2011**, *43*, 984−992.
(53) Leiro, J. A.; Heinonen, M. H.; Laiho, T.; Batirev, I. G. Core-Level Xps Spectra of Fullerene, Highly Oriented Pyrolitic Graphite, and Glassy Carbon. *J. Electron Spectrosc. Relat. Phenom.* **2003**, *128*, 205−213.
(54) Kumar, P. V.; Bernardi, M.; Grossman, J. C. The Impact of Functionalization on the Stability, Work Function, and Photoluminescence of Reduced Graphene Oxide. *ACS Nano* **2013**, *7*, 1638−1645.
(55) Scholl, A.; Zou, Y.; Jung, M.; Schmidt, T.; Fink, R.; Umbach, E. Line Shapes and Satellites in High-Resolution X-Ray Photoelectron Spectra of Large Pi-Conjugated Organic Molecules. *J. Chem. Phys.* **2004**, *121*, 10260−10267.
(56) Crenshaw, M. L.; Banna, M. S. A Study of C1s Binding Energies in Some Gaseous Polycyclic Aromatic Hydrocarbons. *J. Electron Spectrosc. Relat. Phenom.* **1989**, *48*, 179−185.
(57) Voigts, F.; Bebensee, F.; Dahle, S.; Volgmann, K.; Maus-Friedrichs, W. The Adsorption of Co_2 and Co on Ca and Cao Films Studied with Mies, Ups and Xps. *Surf. Sci.* **2009**, *603*, 40−49.